MULTISCALE REMODELING MODEL FOR ORTHODONTIC MOVEMENT CONSIDERING CELLULAR CEMENTUM

Emílio Graciliano Ferreira Mercuri, UFPR, mercuri@ufpr.br
Mildred Ballin Hecke, UFPR, mildredhecke@gmail.com
Lídia Carvalho, INESC-TEC e Universidade do Porto (FCUP), Portugal, licasc@gmail.com

Abstract. *Remodeling is responsible for the removal of the micro-damage and consequently the increase in the useful life of a mineralized tissues. The theory chosen in this study to represent the remodeling was the continuum micromechanics. The authors sought to characterize the hierarchical, anisotropic, heterogeneous and multiscale constitutive behaviour of the bone and cementum. A dynamic interaction model was adopted to describe the cellular interactions and the influence of paracrine signaling on the millimeter-sized representative volume element. The homogenization procedure can provide the macroscopic mechanical properties based on the composition of the microstructure of the material. A computer code, entitled Remold 2D, was developed and programmed in MATLAB. The spatial discretization of the two-dimensional geometries was performed using the Finite Element Method and the temporal evolution of biological variables and volume fractions was solved by the fourth-order Runge-Kutta method. The theory was applied in the orthodontic movement of a central incisor. The mechanical stimulus used to trigger cellular activity is the strain energy density at the microscale. The results show the temporal evolution of the microstrain energy density distribution in the bi-dimensional model. This distribution was shown to be in agreement when compared with other models in the literature. The study is a first step in the development of other studies related to the imbalance of bone homeostasis and the use of drugs in the treatment of bone diseases.*

Keywords: *Cementoblasts, Cementoclasts, multiscale, bone remodeling, Orthodontics*

1. INTRODUCTION

Bone tissue is a living organ capable of adapting to the mechanical environment and is characterized as a composite material, because of its complex composition and hierarchical levels of organization. Biological factors that influence the bone removal and replacement balance are diverse, among them are the cells, cytokines, growth factors, hormones, proteins and lipids that interact in this complex local phenomenon that undergoes systemic influences and external stimuli.

Due to the enormous social impact caused by diseases such as osteoporosis and the failure of implants and prostheses, advances in theoretical understanding and computational simulation of bone remodeling are of great importance (Cowin, 1986).

The objective of this work is to apply a constitutive model for mineralized tissues, using multiscale theory. The mathematical formulation is based on the micromechanics of the continuum and the biological processes are described by a cellular interaction model (between osteoclasts, osteoblasts, cementoclasts and cementoblasts). As specific objectives we can list:

(i) develop a model for the interaction of cementoblasts and cementoclasts;

(ii) perform the coupling of the elastic micromechanical constitutive model with the time evolution model of cellular concentrations and densities. The result of this coupling is a transient analysis of the evolution of the density distribution (bone volume fraction);

(iii) apply the developed theory (mechanical and biological coupling) for bone remodeling in orthodontic movement.

2. MATHEMATICAL MODEL FOR CELLS INTERACTIONS

Lemaire *et al.* (2004) presented a system of ordinary differential equations that modeled cellular interactions. In its model, seven cell groups were considered, representing the different temporal stages of the bone remodeling process. However, many aspects of cellular interactions have not been described by their model and remain open. In this sense, Pivonka *et al.* (2008) made an adaptation to the previous model, adding a new differential equation to describe the variation of bone volume. In the same sequence, Scheiner *et al.* (2012) introduced new functions that allow changing the sensitivity of the system to mechanical signals, such as strain energy. The main influence of deformation energy is on the

proliferation of osteoblasts and the production of RANKL (protein that controls cell proliferation). Although not all were considered in this study, the cells micromechanical environment is a dynamic milieu of biophysical stimuli that includes strain, stress, shear, pressure, fluid flow, streaming potentials and acceleration (Thompson, *et al.* 2012).

It was considered in the simulation that the cells can belong either to bone tissue or cellular cementum. These are the only dynamic materials which can change properties. The tooth root cementum is a thin, mineralized tissue covering the root dentin that is present primarily as acellular cementum on the cervical root and cellular cementum covering the apical root (Foster, 2012). Cells: OB_u represents progenitors of undifferentiated osteoblasts or progenitors of undifferentiated cementoblasts, OB_p indicates the precursors of osteoblasts or precursors of cementoblasts, OB_a is the symbol for active osteoblasts or active cementoblasts, OC_p denotes the pre-osteoclasts or pre-cementoclasts and OC_a represents the active osteoclast or active cementoclast. Cell populations are expressed in terms of concentrations C_i defined as the number of cells in a volume element representative of the bone divided by its volume, the subscript i indicates the type of cell. The unit used for concentrations is pM, Picomolar (10^{-12} mol/dm^3).

The concentrations of blastic or clast cells increase or reduce the volume fractions f_i, respectively. The fraction is defined by $f_i = V_i/V_{\text{total}}$, where V_i represents the volume fraction of phase i and V_{total} the total volume, $V_{\text{total}} = \sum_i V_i$. For cortical or trabecular bone and for the cementum, the following expression (Eq. 1) is valid:

$$f_{\text{exvas}} + f_{\text{vas}} = 1 \tag{1}$$

where f_{exvas} is the volume fraction of the extravascular bone matrix or extravascular cement matrix and f_{vas} is the volume fraction of haversian canals or intertrabecular space or cementum vascularity.

The system of coupled ordinary differential equations of the model is presented in Equations (2-5):

$$\frac{\mathrm{d}C_{\mathrm{OB}_p}}{\mathrm{d}t} = \mathscr{D}_{\mathrm{OB}_u} C_{\mathrm{OB}_u} \pi^{\text{TGF-}\beta}_{\text{act,OB}_u} + \mathscr{P}_{\mathrm{OB}_p} C_{\mathrm{OB}_p} \Pi_{\varepsilon_{\text{bm}}} - \mathscr{D}_{\mathrm{OB}_p} C_{\mathrm{OB}_p} \pi^{\text{TGF-}\beta}_{\text{rep,OB}_p} \tag{2}$$

$$\frac{\mathrm{d}C_{\mathrm{OB}_a}}{\mathrm{d}t} = \mathscr{D}_{\mathrm{OB}_p} C_{\mathrm{OB}_p} \pi^{\text{TGF-}\beta}_{\text{rep,OB}_p} - \mathscr{A}_{\mathrm{OB}_a} C_{\mathrm{OB}_a} \tag{3}$$

$$\frac{\mathrm{d}C_{\mathrm{OC}_a}}{\mathrm{d}t} = \mathscr{D}_{\mathrm{OC}_p} C_{\mathrm{OC}_p} \pi^{\text{RANKL}}_{\text{act,OC}_p} - \mathscr{A}_{\mathrm{OC}_a} C_{\mathrm{OC}_a} \pi^{\text{TGF-}\beta}_{\text{act,OC}_a} \tag{4}$$

$$\frac{\mathrm{d}f_{\text{exvas}}}{\mathrm{d}t} = k_{\text{form}} C_{\mathrm{OB}_a} - k_{\text{res}} C_{\mathrm{OC}_a} \tag{5}$$

where $\mathscr{D}_{\mathrm{OB}_u}$, $\mathscr{D}_{\mathrm{OB}_p}$ and $\mathscr{D}_{\mathrm{OC}_p}$ are the rates of differentiation of progenitors of undifferentiated cells. $\mathscr{P}_{\mathrm{OB}_p}$ is the proliferation rate of pre-osteoblasts or pre-cementoblasts. $\mathscr{A}_{\mathrm{OB}_a}$ and $\mathscr{A}_{\mathrm{OC}_a}$ represent the apoptosis rates of active cells. $\pi^{\text{TGF-}\beta}_{\text{act,OB}_u}$, $\pi^{\text{TGF-}\beta}_{\text{act,OC}_a}$ and $\pi^{\text{TGF-}\beta}_{\text{rep,OB}_p}$ are the activation and inhibition functions that regulate the differentiation of osteoblasts and apoptosis of osteoclasts by TGF-β, while $\pi^{\text{RANKL}}_{\text{act,OC}_p}$ is the activation function regulating the differentiation of osteoclasts by the RANK-RANKL-OPG signaling pathway. The parameters k_{form} and k_{res}represent the rates of bone formation and resorption, ie, percentage of bone turnover per pM of cells per time. The mechanorregulation function $\Pi_{\varepsilon_{\text{bm}}}$ will be discussed in the next subsection. The Figure 1 illustrates the model, for more details see Mercuri *et al.* (2014).

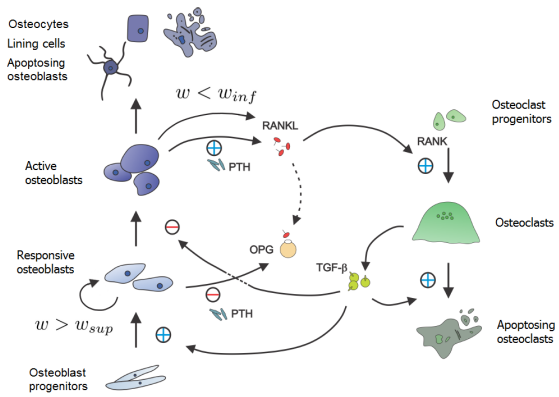

Figure 1. Structure of the model (Mercuri *et al.*, 2014)

3. MICROMECHANICS AND SELF-REGULATION OF MECHANICAL STIMULUS

Mechano-bio-regulation of the mechanical stimulus is the ability of cells to act as microdeformation sensors at the level of the extravascular matrix and to send signals for other cells to work on bone or cementum remodeling. The microstrain energy density at the microscale is the stimulus for a cell to produce cytokines that, once signaled, stimulate cellular differentiation. Figure 2 illustrates the mathematical modeling of biomechanical regulation functions.

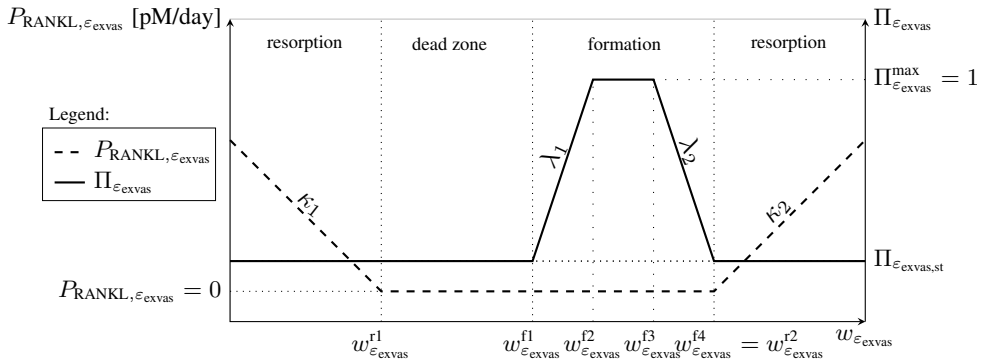

Figure 2. Regulation diagram of cell proliferation based on the MicroStrain Energy Density (MSED).

The biomechanical regulation functions, $\Pi_{\varepsilon_{\text{exvas}}}$ e $P_{\text{RANKL},\varepsilon_{\text{exvas}}}$, are shown in Eq. 6 and Eq. 8. The function of anabolic mechano-regulation (bone or cement formation), $\Pi_{\varepsilon_{\text{exvas}}}$, is defined as:

$$\Pi_{\varepsilon_{\text{exvas}}} = \begin{cases} \Pi_{\varepsilon_{\text{exvas,st}}} & \text{if} \quad w_{\varepsilon_{\text{exvas}}} < w^{f1}_{\varepsilon_{\text{exvas}}} \\ \Pi_{\varepsilon_{\text{exvas,st}}} \left[1 + \lambda_1 \left(\frac{w_{\varepsilon_{\text{exvas}}}}{w^{f1}_{\varepsilon_{\text{exvas}}}} - 1\right)\right] & \text{if} \quad w^{f1}_{\varepsilon_{\text{exvas}}} < w_{\varepsilon_{\text{exvas}}} < w^{f2}_{\varepsilon_{\text{exvas}}} \\ \Pi^{\text{max}}_{\varepsilon_{\text{exvas}}} & \text{if} \quad w^{f2}_{\varepsilon_{\text{exvas}}} < w_{\varepsilon_{\text{exvas}}} < w^{f3}_{\varepsilon_{\text{exvas}}} \\ \lambda_2 \left(w_{\varepsilon_{\text{exvas}}} - w^{f3}_{\varepsilon_{\text{exvas}}}\right) + \Pi^{\text{max}}_{\varepsilon_{\text{exvas}}} & \text{if} \quad w^{f3}_{\varepsilon_{\text{exvas}}} < w_{\varepsilon_{\text{exvas}}} < w^{f4}_{\varepsilon_{\text{exvas}}} \\ \Pi_{\varepsilon_{\text{exvas,st}}} & \text{if} \quad w_{\varepsilon_{\text{exvas}}} > w^{f4}_{\varepsilon_{\text{exvas}}} \end{cases} \tag{6}$$

where $\Pi_{\varepsilon_{\text{exvas,st}}}$ is the steady state value of the anabolic mechano-regulation function. The constants λ_1 and λ_2 represent the inclinations of the straight lines (Figure 2) and $\Pi^{\text{max}}_{\varepsilon_{\text{exvas}}}$ is the maximum value of the anabolic mechano-regulation function (blastic proliferation is limited, $\Pi^{\text{max}}_{\varepsilon_{\text{exvas}}} = 1$). The values of $w^{f1}_{\varepsilon_{\text{exvas}}}, w^{f2}_{\varepsilon_{\text{exvas}}}, w^{f3}_{\varepsilon_{\text{exvas}}}$ and $w^{f4}_{\varepsilon_{\text{exvas}}}$ represent the deformation energy densities at the microscale in the beginning, middle, and end of the formation phase (or blastic proliferation). The constant λ_2 (Eq. 7) can be written according to the other variables:

$$\lambda_2 = \frac{\Pi_{\varepsilon_{\text{exvas,st}}} - \Pi^{\text{max}}_{\varepsilon_{\text{exvas}}}}{w^{f4}_{\varepsilon_{\text{exvas}}} - w^{f3}_{\varepsilon_{\text{exvas}}}} \tag{7}$$

The function of catabolic mechano-regulation (bone or cement resorption), $P_{\text{RANKL},\varepsilon_{\text{exvas}}}$, is defined as:

$$P_{\text{RANKL},\varepsilon_{\text{exvas}}} = \begin{cases} \kappa_1 \left(1 - \frac{w_{\varepsilon_{\text{exvas}}}}{w^{r1}_{\varepsilon_{\text{exvas}}}}\right) & \text{if} \quad w_{\varepsilon_{\text{exvas}}} < w^{r1}_{\varepsilon_{\text{exvas}}} \\ 0 & \text{if} \quad w^{r1}_{\varepsilon_{\text{exvas}}} < w_{\varepsilon_{\text{exvas}}} < w^{r2}_{\varepsilon_{\text{exvas}}} \\ \kappa_2 \left(\frac{w_{\varepsilon_{\text{exvas}}}}{w^{r2}_{\varepsilon_{\text{exvas}}}} - 1\right) & \text{if} \quad w_{\varepsilon_{\text{exvas}}} > w^{r2}_{\varepsilon_{\text{exvas}}} \end{cases} \tag{8}$$

where κ_1 and κ_2 are the slopes of dashed lines (Figure 2). The values $w^{r1}_{\varepsilon_{\text{exvas}}}$ and $w^{r2}_{\varepsilon_{\text{exvas}}}$ represent the initial and final microstrain energy densities of the reabsorption phase (or catabolic phase), that is, in which clastic activity prevails. Table 1 shows the values of the variables used in the numerical simulation, besides the first two parameters, the others were calibrated by the authors. For more information about the model please consult Mercuri (2013).

4. MATERIALS AND METHODS

The algorithm of the Remold 2D developed code represents the coupling of a micromechanical model with the biological model of cellular interaction. The spatial discretization of the geometry was performed by the Finite Element Method

Table 1. Parameters of the model

Symbol	Value	Unit	Description
$\Pi_{\varepsilon_{\text{exvas,st}}}$	$^{\ddagger}0.5 \times 10^{0}$	–	equilibrium value (steady state) for $\Pi_{\varepsilon_{\text{exvas}}}$
$\Pi^{\text{max}}_{\varepsilon_{\text{exvas}}}$	$^{\ddagger}1.0 \times 10^{0}$	–	max. of the anabolic mechano-regulation function
λ_1	2.0×10^{-4}	–	slope 1 of the formation line
λ_2	1.0×10^{16}	–	slope 2 of the formation line
κ_1	1.0×10^{3}	–	slope 1 of the resorption line
κ_2	1.0×10^{1}	–	slope 2 of the resorption line
$w^{\text{r1}}_{\varepsilon_{\text{exvas}}}$	2.0×10^{2}	Pa	lower bone matrix MSED*
$w^{\text{r2}}_{\varepsilon_{\text{exvas}}}$	1.0×10^{16}	Pa	upper bone matrix MSED*
$w^{\text{f1}}_{\varepsilon_{\text{exvas}}}$	9.8×10^{6}	Pa	bone or cement matrix MSED* at the beginning of the formation phase
$w^{\text{f2}}_{\varepsilon_{\text{exvas}}}$	7.0×10^{7}	Pa	bone or cement matrix MSED* for maximum formation 1
$w^{\text{f3}}_{\varepsilon_{\text{exvas}}}$	1.2×10^{8}	Pa	bone or cement matrix MSED* for maximum formation 2
$w^{\text{f4}}_{\varepsilon_{\text{exvas}}}$	1.0×10^{16}	Pa	bone or cement matrix MSED* at the end of the formation phase

Legend: ‡ Scheiner (2012) Model Parameters. *MicroStrain Energy Density (MSED).

and the temporal evolution of biological variables and bone density (volume fractions) was solved by the Runge-Kutta method. This model was used to study bone remodeling around a frontal incisor.

The geometric model was obtained from the scanning of a radiograph, it can be seen in the left image of Fig. 3. The two-dimensional model represents a cut in the mesio-distal direction, in the middle section of the central incisor. For this reason, the visualization of the orthodontic bracket, where the forces usually applied, was omitted. The finite element model consists of 12,474 elements and 25,283 nodes. A force of 2.0 N (Mercuri, 2013) in the horizontal direction was applied to simulate the orthodontic load (right image of Fig. 3).

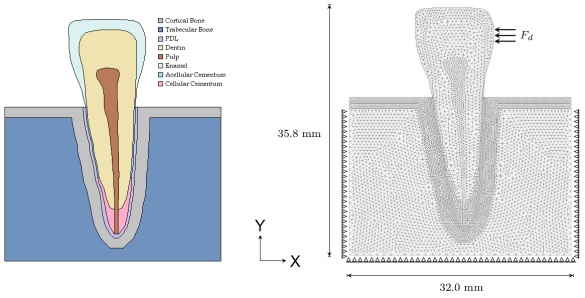

Figure 3. Left - Geometric model; Right - Finite element mesh.

Table 2 shows the values of the constitutive constants used in the simuation of the orthodontic movement.

Table 2. Macroscale constitutive properties of the frontal incisor model.

Material	Young's Modulus	Poisson Coefficient
trabecular bone[a]	1.37 GPa	0.30
cortical bone[a]	13.70 GPa	0.30
periodontal ligament[b]	0.68 MPa	0.47
dentin[a]	18.60 GPa	0.31
pulp[a]	1.37 GPa	0.30
enamel[b]	20.00 GPa	0.30
cementum[c]	30.00 GPa	0.30

[a] Boccaccio *et al.*, (2006); [b] Park *et al.*, (2017); [c] Srivicharnkul *et al.*, (2005)

To illustrate the response of the model in the microscale was adopted the time step h = 0.1 day for 800 iterations, totalling 80 days of simulation of the evolution of cellular concentrations. The RK4 method is a fourth-order method, meaning that the local truncation error is on the order of $O(h^5)$.

The computational work was divided into three stages: pre-processing, processing and post-processing. In preprocessing the overall characteristics of the analysis are defined, such as the number of load cycles, the finite element mesh and the number of Gaussian points. In all analyses, triangular plane elements, with 6 Gauss points, were adopted in a plane

stress state. The finite element mesh was generated with Ansys® software and imported into Matlab® software for the processing and post-processing stages.

The macroscopic properties of the materials, such as the modulus of elasticity and the Poisson coefficient, were chosen according to the literature (Boccaccio *et al.*, 2006; Park *et al.*, 2017; Srivicharnkul *et al.*, 2005). In the pre-processing, three input files were read by the program: the first file has the coordinates of the nodes; the second, the connectivity of the elements of the finite element mesh, and the third contained all contour nodes, for boundary conditions information, i.e. distributed forces (Neumann) and null displacement (Dirichlet). In the processing stage all model calculations were performed. The numerical application consisted of a transient two-dimensional analysis of the variation of the constitutive properties of bone, volume fractions and cell populations in load cases each day, representing cycles of bone remodeling. In each load case a static structural analysis was performed, together with the solution of the temporal evolution of the coupled model of differential equations of the cellular dynamics. During the initial cycle a purely elastic mechanical analysis was performed. The elementary stiffness matrices are allocated in the global stiffness matrix and the force vectors and null displacement contour conditions were considered. The system of algebraic equations was solved and the nodal displacements were obtained, a procedure that was performed in each subsequent remodeling cycle.

Table 3 shows the volume fractions adopted in the analysis for the different materials with micromechanical behaviour. It was found a great variability in the value of the vascular volume fraction of the materials in the literature (Cooper *et al.*, 2007; Scheiner *et al.*, 2016; Padilla *et al.*, 2008; Boutroy *et al.*, 2005; Boutroy *et al.*, 2011; Milutinovic-Nikolic *et al.*, 2007). Therefore the range of variability (minimum and maximum values) found in the articles of vascular volume fraction are shown in Table 3. The table also shows the initial value for the vascular volume fraction adopted in the simulation.

Table 3. Volume Fraction of the materials with micromechanical behaviour

Material	f_{vas} **range**	f_{vas}
cortical bone[a]	$0.050 - 0.300$	0.17
trabecular bone[b]	$0.500 - 0.900$	0.70
cementum[c]	$0.007 - 0.158$	0.08

[a] (Cooper *et al.*, 2007, Scheiner *et al.*, 2016); [b] (Padilla *et al.*, 2008, Boutroy *et al.*, 2005, Boutroy *et al.*, 2011, Scheiner *et al.*, 2016); [c] (Milutinovic-Nikolic *et al.*, 2007)

5. RESULTS AND DISCUSSION

Figure 4 shows the micromechanical stimulus in the elements which belong to the periodontal ligament on days 1 and 10 of simulation. The intensity of the mechanical stimulus differs in the cortical bone and the periodontal ligament, however we chose to illustrate the variation in the ligament because of the important role that this connective tissue has during tooth movement.

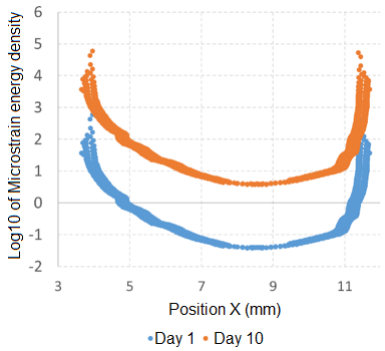

Figure 4. Distribution of the microstrain energy density in the Periodontal Ligament for days 1 and 10

At the beginning of the simulation the vascular volume fraction of the micromechanical behaviour materials were set equal the adopted values of Table 3. The results of the evolution of the volume fraction in the cortical bone show that the regions where the volume fraction of the bone matrix decreased are mostly in state of compressive stresses and the regions where the volume fraction increased are mostly in traction stress state. These results are in agreement with the theory that explains the dental movement, described by Reitan (2007).

6. CONCLUSION

The application of the micromechanical theory of the continuum with the model of cellular interaction in the microscale allowed to develop a methodology to estimate the bone remodeling, exploring aspects of the bone microstructure. The coupling result of the micromechanical and biological models provides a research tool for the transient analysis of the evolution of the distribution of bone density due to the action of osteoblasts, osteoclasts, cementoblasts and cementoclasts.

7. REFERENCES

BOCCACCIO, A., LAMBERTI, L., PAPPALETTERE, C., CARANO, A., & COZZANI, M. (2006). Mechanical behavior of an osteotomized mandible with distraction orthodontic devices. **Journal of Biomechanics**, 39(15), 2907-2918.

BOUTROY S, BOUXSEIN M, MUNOZ F, DELMAS P (2005) In vivo assessment of trabecular bone microarchitecture by high-resolution peripheral quantitative computed tomography. **J Clin Endocrinol Metab** 90(12):6508-6515.

BOUTROY S, VILAYPHIOU N, ROUX J-P, DELMAS P, BLAIN H, CHAPURLAT R, CHAVASSIEUX P (2011) Comparison of 2D and 3D bone microarchitecture evaluation at the femoral neck, among postmenopausal women with hip fracture or hip osteoarthritis. **Bone** 49(5):1055-1061.

COOPER D, THOMAS C, CLEMENT J, TURINSKY A, SENSEN C, HALLGRÍMSON B (2007) Age-dependent change in the 3D structure of cortical porosity at the human femoral midshaft. **Bone** 40(4):957-965.

COWIN, S.C. (1986) Wolff's law of trabecular architecture at remodeling equilibrium. **Journal of Biomechanical Engineering**, v. 108, p. 83-88.

FOSTER, B. L. (2012). Methods for studying tooth root cementum by light microscopy. **International journal of oral science**, 4(3), 119-128.

LEMAIRE, V., TOBINA, F.L., GRELLERA, L.D., CHOA, C.R., AND SUVAB, L.J. (2004) Modeling the interactions between osteoblast and osteoclast activities in bone remodeling. **Journal of Theoretical Biology**, 229, 293-309.

MERCURI, E. G. F. (2013). **Modelagem multiescala de tecidos mineralizados considerando a micromecânica da dinâmica celular** (Tese de Doutorado). Programa de Pós-Graduação em Métodos Numéricos em Engenharia (PPGMNE), Universidade Federal do Paraná (UFPR).

MERCURI, E. G. F., DANIEL, A. L., MACHADO, R. D., & HECKE, M. B. (2014) Application of a multi-scale mechanobiological model for bone remodeling. **Journal of Medical Imaging and Health Informatics**, 4(1), 142-146.

MILUTINOVIĆ-NIKOLIĆ, A. D., MEDIĆ, V. B., & VUKOVIĆ, Z. M. (2007). Porosity of different dental luting cements. **Dental Materials**, 23(6), 674-678.

PADILLA F, JENSON F,BOUSSONV, PEYRIN F, LAUGIER P (2008) Relationships of trabecular bone structure with quantitative ultrasound parameters: in vitro study on human proximal femur using transmission and backscatter measurements. **Bone** 42(6):1193-1202.

PARK, J. H., BAYOME, M., ZAHROWSKI, J. J., & KOOK, Y. A. (2017). Displacement and stress distribution by different bone-borne palatal expanders with facemask: A 3-dimensional finite element analysis. **American Journal of Orthodontics and Dentofacial Orthopedics**, 151(1), 105-117.

PIVONKA, P., ZIMAK, J., SMITH, D.W., GARDINER, B.S., DUNSTAN, C.R., SIMS, N.A., MARTIN, T.J., and MUNDY, G. (2008) Model structure and control of bone remodeling: A theoretical study. **Bone**, 43, 249-263.

REITAN, K. (2007) The tissue reaction as related to the functional factor. **The European Journal of Orthodontics**, 29, 58-64.

SCHEINER, S., PIVONKA, P., HELLMICH, C., and SMITH, D.W. (2012) Mechanobiological regulation of bone remodeling - Theoretical development of a coupled systems biology-micromechanical approach. **ArXiv e-prints.**

SCHEINER S, PIVONKA P, HELLMICH C (2016) Poromicromechanics reveals that physiological bone strains induce osteocyte-stimulating lacunar pressure. **Biomech Model Mechanobiol** 15:9-28;

SRIVICHARNKUL, P., KHARBANDA, O. P., SWAIN, M. V., PETOCZ, P., & DARENDELILER, M. A. (2005). Physical properties of root cementum: Part 3. Hardness and elastic modulus after application of light and heavy forces. **American journal of orthodontics and dentofacial orthopedics**, 127(2), 168-176.

THOMPSON, W. R., RUBIN, C. T., & RUBIN, J. (2012). Mechanical regulation of signaling pathways in bone. **Gene** 503(2): 179-193.

8. ACKNOWLEDGEMENTS

This work is financed by FEDER Funds through the Competitiveness and Internationalization Operational Program - COMPETE 2020 under the project "POCI-01-0145-FEDER-006961" and by National Funds through FCT - Foundation for Science and Technology through the project UID / EEA / 50014/2013.

9. INFORMATION RESPONSABILITIES

The authors are solely responsible for the information included in this work.